Supporting Information for

ORIGINAL ARTICLE

Multi-responsive nanotheranostics with enhanced tumor penetration and oxygen self-producing capacities for multimodal synergistic cancer therapy

Shuangquan Gou[a,b,c,†], Nanxi Chen[b,†], Xiaoai Wu[d,†], Menghang Zu[b,c], Shixiong Yi[b], Binwu Ying[e,*], Fangyin Dai[b], Bowen Ke[a,*], Bo Xiao[b,c,*]

[a]*Laboratory of Anesthesiology & Critical Care Medicine, Department of Anesthesiology, West China Hospital, Sichuan University, Chengdu 610041, China*

[b]*State Key Laboratory of Silkworm Genome Biology, College of Sericulture, Textile and Biomass Sciences, Southwest University, Chongqing 400715, China*

[c]*Chongqing Key Laboratory of Soft-Matter Material Chemistry and Function Manufacturing, School of Materials and Energy, Southwest University, Chongqing 400715, China*

[d]*Department of Nuclear Medicine, West China Hospital, Sichuan University, Chengdu 610041, China*

[e]*Department of Laboratory Medicine, West China Hospital, Sichuan University, Chengdu 610041, China*

Received 5 March 2021; received in revised form 5 May 2021; accepted 26 May 2021

[*]Corresponding authors. Tel.: + 86 23 68254762 (Bo Xiao); + 86 28 85188632 (Bowen Ke); + 86 28 85423559 (Binwu Ying).

E-mail addresses: bxiao@swu.edu.cn (Bo Xiao), bowenke@scu.edu.cn (Bowen Ke), yingbinwu@scu.edu.cn (Binwu Ying).

[†]These authors made equal contributions to this work.

Experimental details

1.1. Materials

Silkworm cocoons were provided by the State Key Laboratory of Silkworm Genome Biology, Southwest University (Chongqing, China). Sodium acetate and aniline were obtained from Tianjin Bodi Chemical Co., Ltd. (Tianjin, China). Ethanol, methanol, and dichloromethane (DCM) were purchased from Chengdu Cologne Chemical Co., Ltd. (Chengdu, Sichuan, China). Ether, toluene, and hydrochloric acid were from Sichuan Xilong Science Co., Ltd. (Chengdu, Sichuan, China). *N*,*N*-dimethylformamide, cyclohexanone, and ethyl acetate were supplied by Tianjin Zhiyuan Chemical Reagent Co., Ltd. (Tianjin, China). 1,3-Dibromopropane, 1,3-propane sultone, and 4-hydroxybenzoic acid were obtained from Energy Chemical (Shanghai, China). Phosphorus oxychloride was obtained from Shandong West Asia Chemical Industry Co., Ltd. (Linyi, Shandong, China). 2,3,3-Trimethylindolenine was obtained from Adamas reagent co., Ltd. (Shanghai, China). DOX, H_2O_2, GSH, dimethyl sulfoxide, and Triton X-100 were obtained from Sigma–Aldrich (St. Louis, MO, USA). SOSG was from Shanghai Sangon Biological Engineering Technology and Services Company (Shanghai, China). BSP, chlorpromazine, MβCD, and cyclosporin A was supplied by Aladdin (Shanghai, China). MTT and DAPI were supplied by Invitrogen (Eugene, OR, USA). Apoptotic assay kits and liver and kidney toxicity assay kits were from Nanjing Jiancheng Bioengineering Institute (Nanjing, China). Lyso-tracker, Mito-tracker, and buffered formalin (10%) was provided by Thermo Fischer Scientific (Fair Lawn, NJ, USA). Annexin V-FITC/PI apoptosis assay kit, Rho123, DCFH-DA ROS fluorescent probes, H&E, TUNEL, and Ki67 staining kit were supplied by Beyotime Institute of Biotechnology (Nanjing, China). Primary antibody of HIF-1α and FITC-labelled CD31 (FITC-CD31) was purchased from Servicebio (Wuhan, China). Unless otherwise stated, all the organic

solvents and chemical reagents were obtained from commercial sources, and utilized without further purification.

1.2. Synthesis and physicochemical characterization of N770

Sodium acetate (0.73 g, 8.90 mmol) was added to the mixture of compound 1 (3.93 g, 10.94 mmol) and compound 2 (2.5 g, 8.90 mmol) in ethanol (30 mL), and the obtained mixture was refluxed at 80 ^{o}C for 3 h. Subsequently, the reaction mixture was concentrated, and the residue was recrystallized from methanol/ether to afford compound 3 (3.5 g, crude) as a deep blue solid. Sodium acetate (380 mg, 4.64 mmol) was added to the mixture of compound 3 (3.5 g, 5.88 mmol) and compound 4 (1.8 g, 4.33 mmol) in ethanol (20 mL), and the reaction was carried out at 80 ^{o}C for 3 h. Finally, the reaction mixture was concentrated, and the residue was purified by flash column chromatography elution with methanol/dichloromethane to afford compound 5 (1.05 g, 32.3% yield) as a dark green solid.

A mixture of 5 (500 mg, 0.66 mmol), EDCI (190 mg, 0.99 mmol), and NHS (114 mg, 0.99 mmol) in DCM (10 mL) was stirred at room temperature for 4 h. The reaction mixture was concentrated and the residue was purified by flash column chromatography elution with methanol-dichloromethane to afford desired product NHS-N770 (290 mg) as a deep green solid.

1.3. Physicochemical characterization of N770-DOX@NPs

NMR spectrum of N770 was recorded on a Varian 400 MHz NMR (Mercury Plus 400, Varian, USA), and trimethylchlorosilane was used as an internal standard. Chemical shifts were reported in ppm from tetramethylsilane with the solvent resonance as the internal standard in $CDCl_3$ solution. ^{1}H NMR (400 MHz, $CDCl_3$) δ 8.45 (d, *J* = 14.5 Hz, 1H), 8.11 (dd, *J* = 17.7, 11.2 Hz, 3H), 7.45 (s, 2H), 7.40 (d, *J* = 7.3 Hz, 1H), 7.31 (d, *J* = 7.2 Hz, 2H), 7.27 (d, *J* = 5.5 Hz, 1H), 7.13 (t, *J* = 7.4 Hz, 1H), 7.02 (d, *J* = 7.9 Hz, 1H), 6.95 (d, *J* = 8.7 Hz, 2H), 6.82 (d, *J* = 14.5 Hz,

1H), 5.91 (d, *J* = 13.5 Hz, 1H), 4.68 – 4.52 (m, 2H), 4.27 – 4.09 (m, 4H), 3.02 (d, *J* = 5.3 Hz, 2H), 2.93 (s, 4H), 2.77 (s, 2H), 2.32 (d, *J* = 5.4 Hz, 2H), 2.17 (s, 4H), 1.80 (s, 2H), 1.70 (d, *J* = 6.7 Hz, 12H). ^{13}C NMR (101 MHz, $CDCl_3$) δ 175.60, 169.76, 168.97, 163.49, 161.36, 150.35, 147.96, 142.61, 141.72, 141.63, 140.82, 140.21, 13.02, 129.68, 129.34, 128.64, 127.09, 126.65, 123.96, 122.17, 117.78, 114.62, 112.49, 109.34, 105.45, 97.95, 64.74, 50.09, 48.41, 47.46, 44.20, 40.32, 28.39, 28.00, 26.77, 26.50, 26.25, 25.78, 24.06, 20.73.

The average particle sizes, PDI, and zeta potentials of NPs were determined by DLS (Zetasier NanoZS, Malvan, UK). The average values were tested using 3 runs, and obtained based on the measurements on repeated NPs.

The loading amounts and encapsulation efficiencies of DOX in NPs were determined using a direct method. In a brief, NPs were completely suspended in DMSO, and sonicated at amplitude of 50% to extract drugs from NPs. Thereafter, the fluorescence intensities of DOX were quantified using a fluorescence spectrophotometer (RF-5301 PC, Shimadzu, Japan). On the other hand, the graft volume and graft efficiency of N770 was measured by an indirect method. The amount of NHS-N770 in the supernatant was quantified using a RF-5301 PC fluorescence spectrophotometer (Shimadzu, Japan). The relevant equations were described as follows:

$$\text{Drug loading} = \frac{\text{Weight of DOX in dry NPs}}{\text{Weight of dry NPs}} \times 100\% \quad (1)$$

$$\text{Encapsulation efficiency} = \frac{\text{Weight of actual DOX in dry NPs}}{\text{Weight of DOX feeded}} \times 100\% \quad (2)$$

$$\text{Graft amount of NIR770} = \frac{\text{Weight of feeded NIR770 - NIR770 amount in supernatant}}{\text{Weight of dry NIR770}} \times 100\% \quad (3)$$

$$\text{Graft efficiency of NIR770} = \frac{\text{Weight of feeded NIR770 - NIR770 amount in supernatant}}{\text{Weight of feeded NIR770}} \times 100\% \quad (4)$$

The UV–Vis absorption spectra of various samples were recorded on a UV–Vis–NIR spectrometer (UV-1800, Shimadzu, Japan). The surface morphology of N770-DOX@NPs was measured using a SEM (JEOL JSM -6510LV, Tokyo, Japan). Briefly, NPs were suspended in water, and a drop of NP suspension was deposited on a cleaned wafer and air-dried before test. The FTIR spectra of various samples were detected using a Bruker EQUINOX 55 FTIR Spectrophotometer (Billerica, MA, USA).

The capacity of RSF-based NPs to catalyze the decomposition of H_2O_2 was determined by direct methods. Briefly, RSF solution, blank NP suspension, and N770-DOX@NP suspension with the same amount of RSF (0.5 mg/mL) were added to H_2O_2 solution (0.5 mmol/L), respectively. Simultaneously, the generation of O_2 in H_2O_2 solution was recorded by dissolved oxygen analyzer (Xiamen Kelungde Env. Engineering Co., Ltd., Xiamen, China).

The CD spectra of RSF, blank NPs, DOX@NPs, and N770-DOX@NPs were recorded on a MOS-500 instrument (Bio-logic, France). The measurements were conducted in a wavelength ranging from 190 to 240 nm at 22 ^{o}C, and NP suspensions were tested in a cell with a path length of 0.1 cm. The CD spectra were further analyzed by CDNN CD spectral deconvolution software to elucidate the variations of the secondary structures of NPs.

1.4. Multi-responsive drug release profiles of N770-DOX@NPs

A dialysis method was applied to study the controlled release profiles of drugs from RSF-based NPs. Briefly, N770-DOX@NPs were dispersed in water (equivalent to 500 μg of DOX), and the suspensions were transferred into dialysis bags (MWCO = 1400 Da). These bags were sealed in both ends, and then immersed in tubes with different releasing media. The tubes were deposited in a water bath shaking at 120 rpm at 37 ^{o}C. At pre-determined time intervals, the releasing

media were taken for measurements, and fresh releasing media were added. DOX amounts in the releasing media were quantified at 488 nm excitation wavelength and 575 nm emission wavelengths using a RF-5301 PC fluorescence spectrophotometer (Shimadzu, Japan).

1.5. Photothermal property of N770-DOX@NPs

The aqueous solutions of free N770 and N770-DOX@NPs with the same N770 concentration (0.5 mg/mL) were subjected to NIR irradiation (808 nm, 1.5 W) for 5 min. The temperature values of these solutions were monitored by digital thermometer during NIR irradiation. And the corresponding thermographic images of the sample-filled cuvettes were captured using an infrared thermal imaging camera (TiS55, Fluke, WA, USA). Four NIR irradiation cycles were performed to characterize the photothermal stability of free N770 and N770-DOX@NPs. Briefly, samples were suspended in deionized water, exposed to NIR irradiation for 5 min, and cooled down to the ambient temperature in each cycle.

1.6. Photodynamic property of N770-DOX@NPs

To evaluate the photodynamic property of samples, SOSG was employed as a probe to quantify the generated amounts of $^1O_2$. Typically, samples with the N770 concentration of 0.1 mg/mL and SOSG (1.5×10^{-6} M) were mixed and irradiated for 5 min (808 nm, 1.5 W/cm^2). The fluorescence intensities of the irradiated solutions were promptly measured at 494 nm excitation wavelength and 530 nm emission wavelength using a RF-5301 PC Fluorescence spectrophotometer (Shimadzu, Japan).

The generated amounts of intracellular ROS were determined using DCFH-DA as a fluorescent probe. Briefly, A549 cells were seeded in 12-well plates at 2×10^5 cells per well and incubated overnight. Subsequently, the complete medium was replaced with a serum-free medium containing free N770 or N770-DOX@NPs, and further incubated for 4 h. Thereafter,

cells were rinsed with cold PBS, fresh media were added to the wells, and cells were irradiated by NIR laser (808 nm, 1.5 W/cm^{-2}) for 5 min. 30 min after the irradiation, DCFH-DA solution (10×10^{-6} M) was added to each well, and further incubated for 30 min. Finally, cells were collected, and their fluorescence intensities were determined by FCM (ACEA Biosciences, Inc., San Diego, USA). The results were normalized as folds compared with the negative control.

1.7. In vitro biocompatibility of N770-DOX@NPs

HUVECs were used to evaluate the biocompatibility of N770-DOX@NPs. Briefly, HUVECs were seeded in 96-well plates at a concentration of 2×10^4 cells per well, and cultured overnight at 37°C. After that, the complete media were replaced with basic media containing various samples. After incubation for 24 or 48 h, cells were rinsed with PBS for 3 times, and incubated with MTT (0.5 mg/mL) for 4 h. Subsequently, MTT-contained medium was discarded, and DMSO was added to each well before spectrophotometric measurements at a wavelength of 570 nm. Cells without treatment were used as a negative control, whereas Triton X-100 (0.5%, *w/v*)-treated cells were used a positive control.

1.8. In vitro subcellular location of N770-DOX@NPs

Subcellular localization of N770-DOX@NPs was determined by co-staining method. Briefly, A549 cells were seeded in 8-well plates at a cell density of 1×10^5 cells per well and cultured overnight at 37 ℃. After that, the complete media were replaced with basic media containing N770-DOX@NPs with a N770 concentration of 50 μg/mL. After co-incubation for different times, lysosome and mitochondria were stained with Lyso-tracker (1: 10,000 diluted with PBS) or Mito-tracker (1: 6000 diluted with PBS) for 30 min, respectively, and nucleus were stained with DAPI. Cells were imaged using a CLSM (Zeiss-800, Germany).

1.9. Penetration profiles of N770-DOX@NPs in MCSs

A549 MCSs were prepared to simulate tumor masses for evaluating the penetration properties of N770-DOX@NPs *in vitro*. Briefly, 50 μL of agarose solution (1%, *w*/*v*) were added to 96-well plates, and A549 cells were seeded at a cell density of 3.0×10^4 cells per well. After incubation for 48 h, MCSs were treated with N770-DOX@NPs (Cy7, 10 μg/mL) with or without NIR irradiation. Laser irradiation groups were carried out with laser (808 nm, 1.5 W/cm^2). Finally, MCSs were rinsed and fixed, and imaged using a CLSM (Zeiss-800, Germany).

1.10. Pro-apoptotic property of N770-DOX@NPs

A549 cells were seeded in 6-well plates at a cell density of 1×10^6 cells per well and cultured overnight at 37 ^{o}C. After that, the complete media were replaced with basic media containing N770-DOX@NPs with various DOX concentrations (4, 6, and 8 μmol/L). After incubation for 4 h, cells were irradiated with NIR laser (808 nm, 1.5 W/cm^2) for 5 min. Four hours after further incubation, cells were collected and co-stained with Annexin V-Alexa FITC and PI for FCM (ACEA Biosciences, USA) analysis.

1.11. Western blotting

A549 cells were seeded in 6-well plates at a cell density of 2×10^6 cells per well. After overnight incubation, cells were co-incubated with various NPs for 4 h. The supernatant was discarded, and cells in the irradiation group was irradiated with NIR Laser (808 nm, 1.5 W/cm^2) for 5 min. After further incubation for 4 h, cells were washed with PBS for 3 times and lysed by RIPA solution. Total proteins were collected and separated by SDS-PAGE. Subsequently, proteins were transferred to PVDF membrane and incubated with primer antibodies overnight at 4 ^{o}C. The transferred member was completely blocked by 5% fat-free milk. After incubation with secondary antibody, proteins were detected by using ECL chemical luminance reagent according to the manufacturer's instructions.

1.12. Multimodal imaging of N770-DOX@NPs

Athymic nude mice with subcutaneous tumor xenograft were used for tumor imaging. When the volumes of tumor xenografts reached 150 mm^3, free N770 or N770-DOX@NPs with equal concentration of N770 (1 mg/kg) were intravenously injected to mice. After injection for different time points (6, 12, 24, 48, and 72 h), FLI of whole bodies and individual organs was performed on a Kodak In-Vivo FX professional Imaging System (CT, USA) equipped with fluorescent filter sets (770/830 nm). The fluorescence intensities of tumors and major organs were calculated using Fusion software to study the biodistribution and retention of free N770 or N770-DOX@NPs in tumors.

For *in vivo* thermal imaging, free N770 or N770-DOX@NPs with an equal concentration of N770 (1 mg/kg) were intravenously injected to mice bearing tumor xenografts. Twenty-four hours after administration, PTI was performed on an infrared thermal imaging camera (TiS55, Fluke) within 5 min laser irradiation (808 nm, 0.8 W/cm^2).

For PAI, mice bearing A549 lung tumor xenografts were intravenously injected with N770-DOX@NPs at a N770 concentration of 1 mg/kg (100 μL). Subsequently, at predetermined time points (12, 24, 48, and 72 h), tumor regions were imaged with an excitation wavelength at 770 nm using a VisualSonics (Vevo 2100; VisualSonics Inc., Ontario, Canada).

In vivo MRI was conducted on mice bearing A549 lung tumor xenograft. At the end of the anti-tumor experiments, all the mice were performed a 1T MRI scanner (NM42-040H-I, Suzhou Niumag Analytical Instrument Corporation, Suzhou, China).

Tumor tissues were extracted after intravenous injection of various samples for 24 h, and embedded in Optimal Cutting Temperature compound. The tissue sections (5 μm) were stained

with DAPI and FITC-CD31. Finally, the sections were imaged using a CLSM (Zeiss-800, Germany).

The DOX concentrations in various samples were quantified by high performance liquid chromatography (HPLC) according to previous reports[1,2].

1.13. Hemolysis assay

Blood was collected from the eyelid posterior sinus vein of BALB/c mice (10 week old) to evaluate the hemocompatbility of NPs. Erythrocytes were harvested by centrifugation at 2500 ×*g* for 10 min, washed 3 times, and suspended in PBS (2%, *v*/*v*). At the same time, NPs were dispersed in PBS and diluted to different drug concentrations. After that, the mixtures of erythrocytes and NPs were incubated for 1 h at 37 ^{o}C prior to centrifugation at 3000 × *g* (KH20R, Changsha, China)for 15 min. Finally, hemoglobin amounts in the supernatants were analyzed by spectrophotometric tests at 570 nm. The untreated erythrocyte suspension was utilized as a negative control, whereas erythrocyte suspension treated with Triton X-100 (1%, *v*/*v*) was used as a positive control.

1.14. Statistical analysis

Data were presented as means ± standard error of the mean (SEM). Statistical analysis was conducted using the student's *t*-test or one-way ANOVA. Statistical significance was represented by $*P < 0.05$ and $**P < 0.01$.

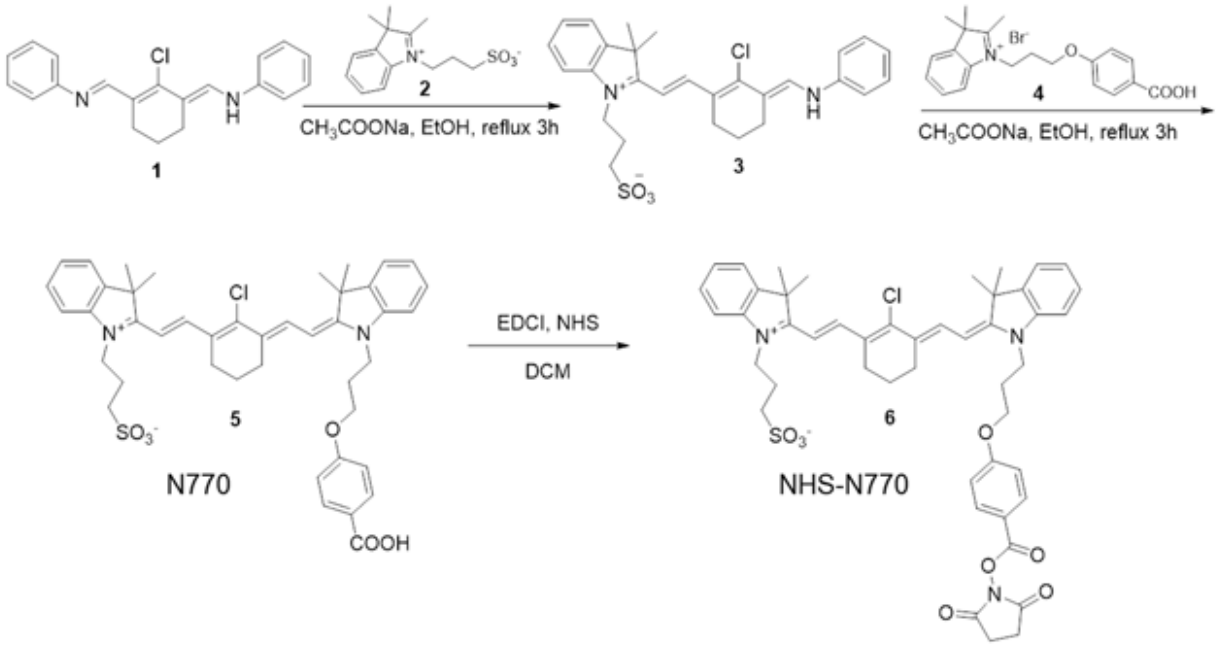

Sheme S1 Synthetic scheme of NHS-N770.

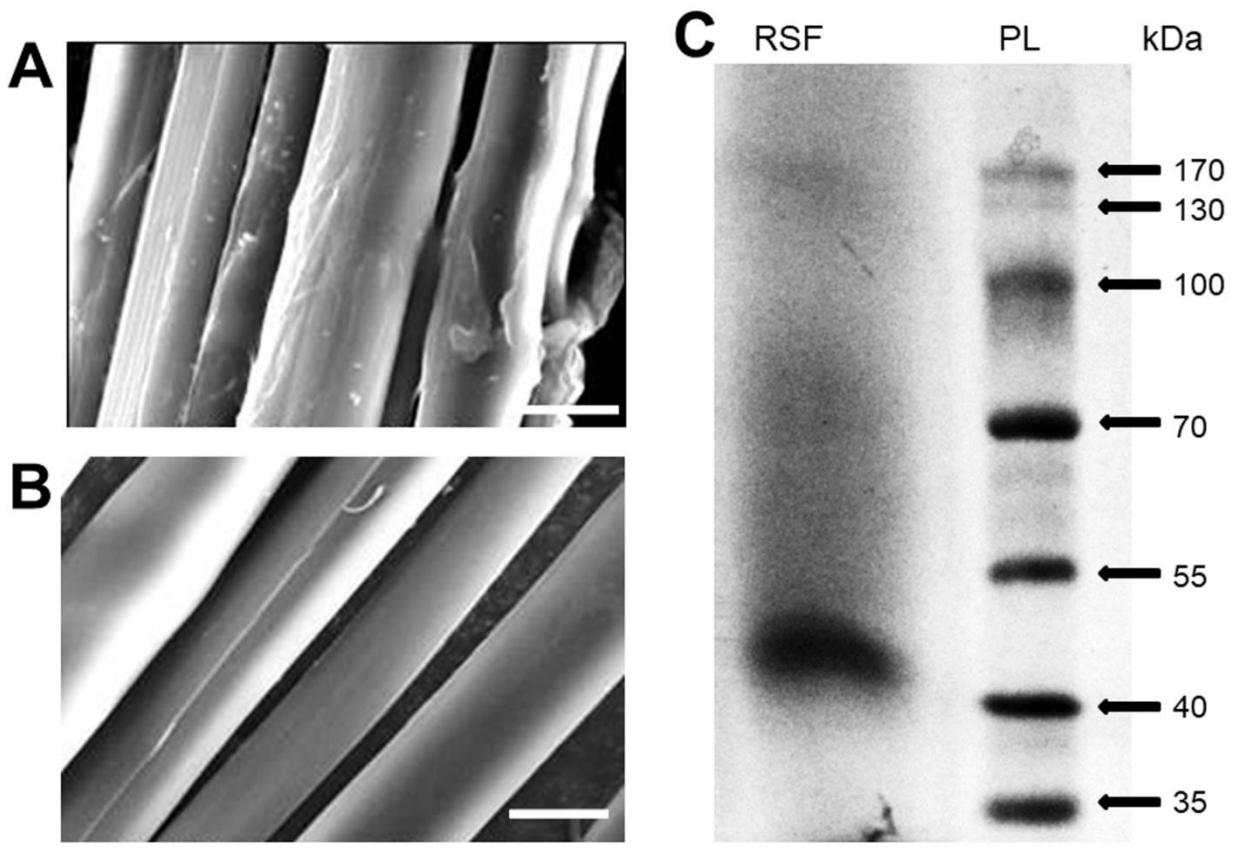

Figure S1 Representative SEM images of (A) non-degummed and (B) degummed silk fibroins. Scale bar is 10 μm. (C) SDS-PAGE of RSF.

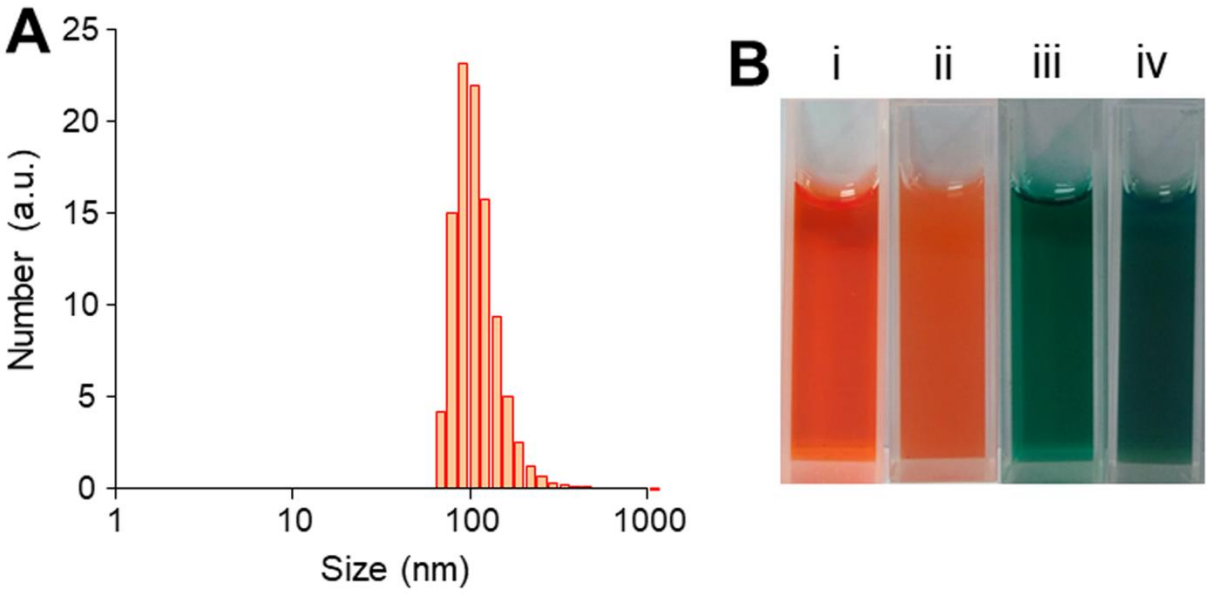

Figure S2 (A) Size distribution of N770-DOX@NPs. (B) Photographs of (i) free DOX solution, (ii) DOX@NP suspension, (iv) free N770 solution, and (v) N770-DOX@NPs.

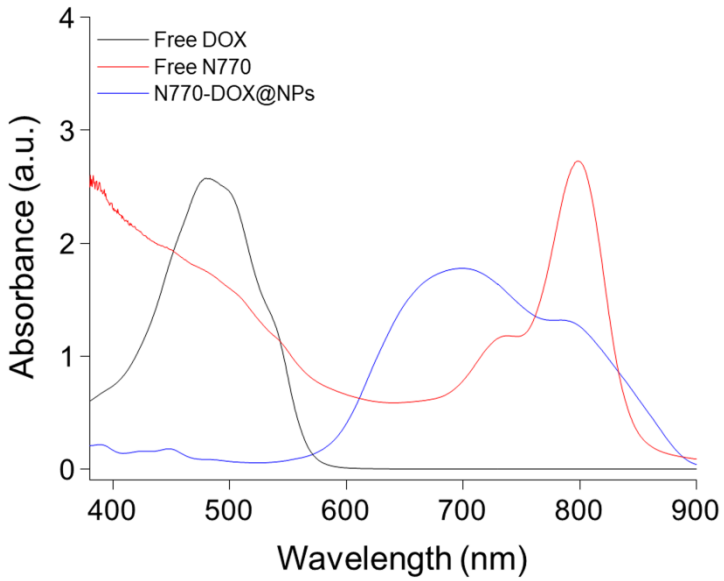

Figure S3 UV–Vis spectra of free N770 solution, free DOX solution, and N770-DOX@NP suspension.

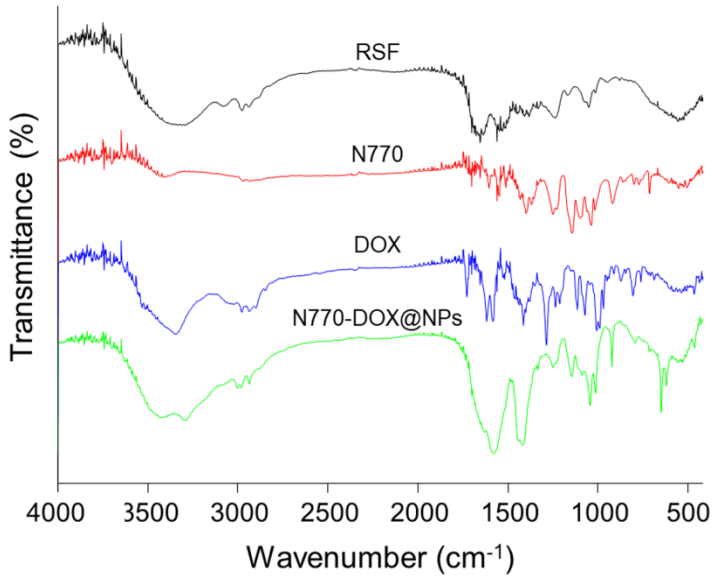

Figure S4 FTIR spectra of RSF, free N770, free DOX, and N770-DOX@NPs.

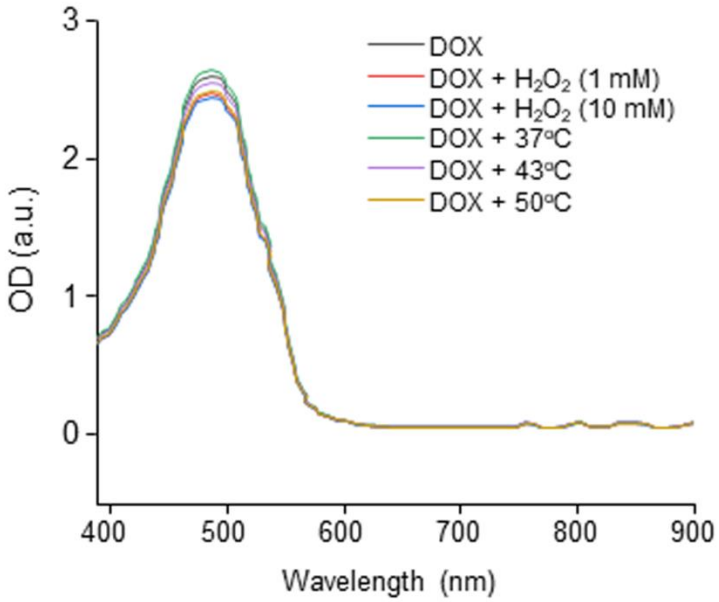

Figure S5 The absorption spectra of DOX solutions receiving various treatments for 7 days.

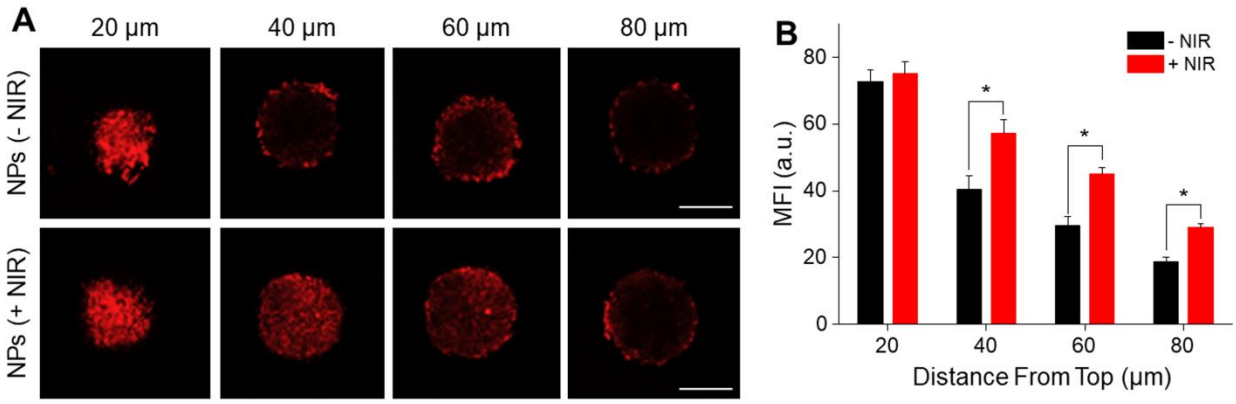

Figure S6 Uptake profiles of NPs by MCSs of 4T1 cells. (A) Penetration profiles and (B) the corresponding quantitative results of N770-DOX@NPs in MCSs with or without NIR laser irradiation. Scale bars represent 100 μm.

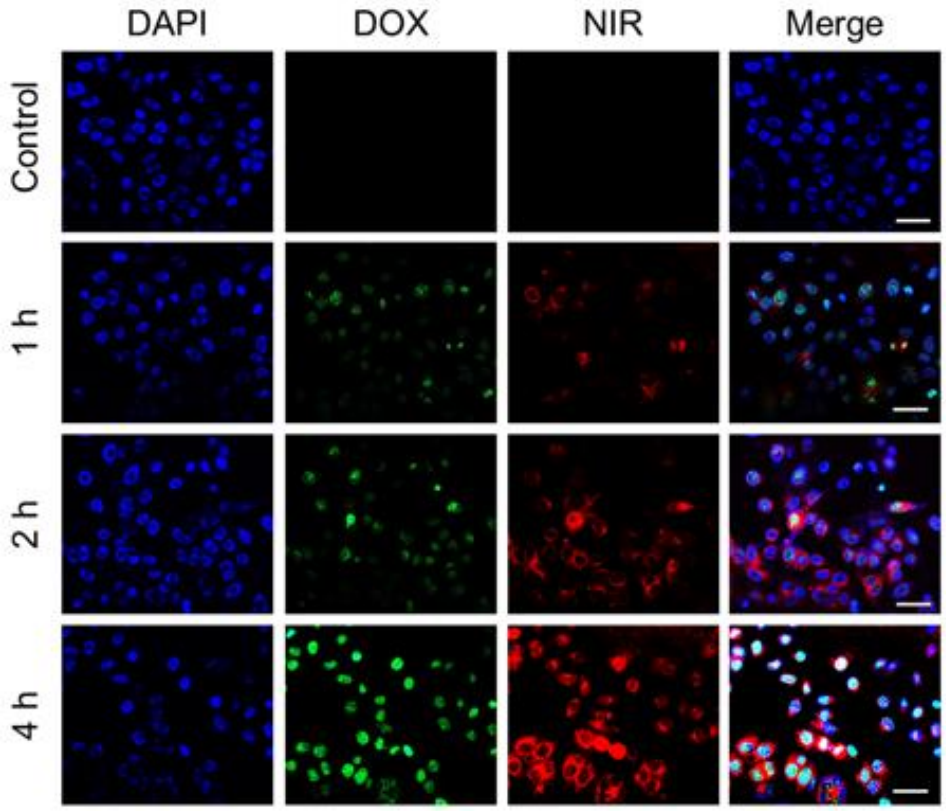

Figure S7 Confocal images of cellular uptake profiles of N770-DOX@NPs in A549 cells at the incubation timepoints of 1, 2, and 4 h, respectively. Nuclei were stained with DAPI (blue). Scale bar is 20 μm.

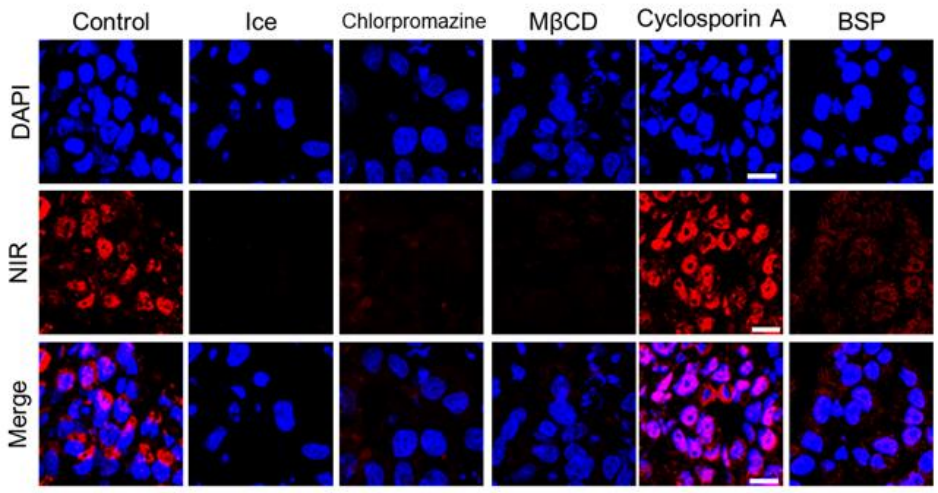

Figure S8 Celllular uptake mechanism of N770-DOX@NPs by A549 cells when intervening with (i) the endocytotic process: chlorpromazine and M*β*CDp; (ii) the energy dependence of the process: ice incubation and OATPs (BSP); and (iii) ABC transporters: ciclosporin A. Scale bar is 10 μm.

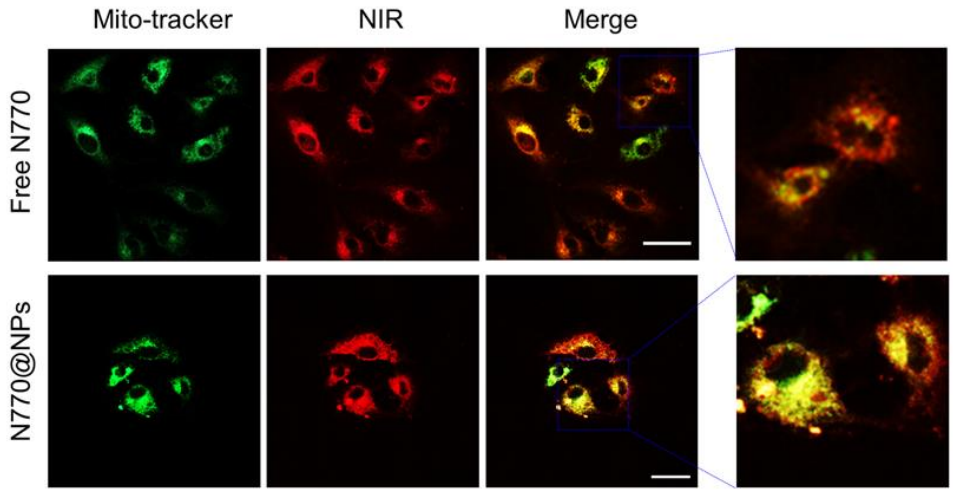

Figure S9 Co-localization profiles of mitochondria and N770-DOX@NPs in A549 cells. Scale bar is 20 μm.

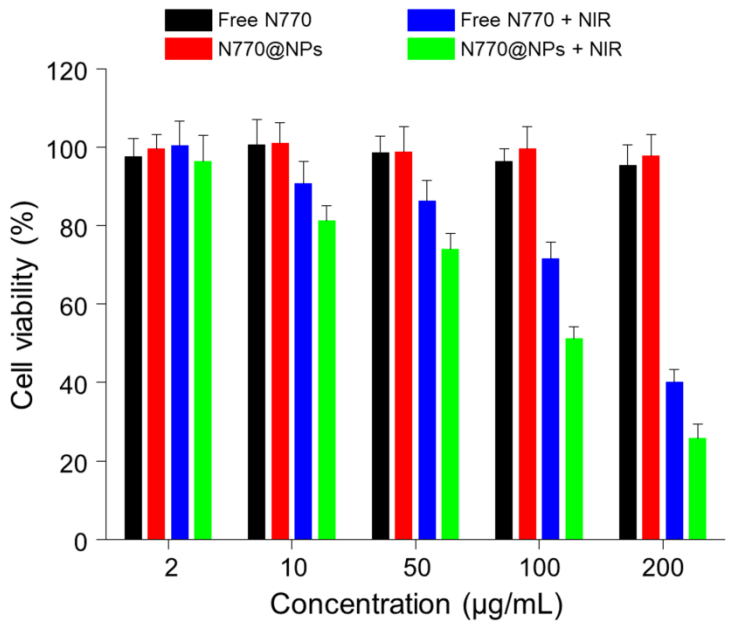

Figure S10 Viabilities of HUVECs receiving different treatments. Data are expressed as mean ± SEM (n = 5).

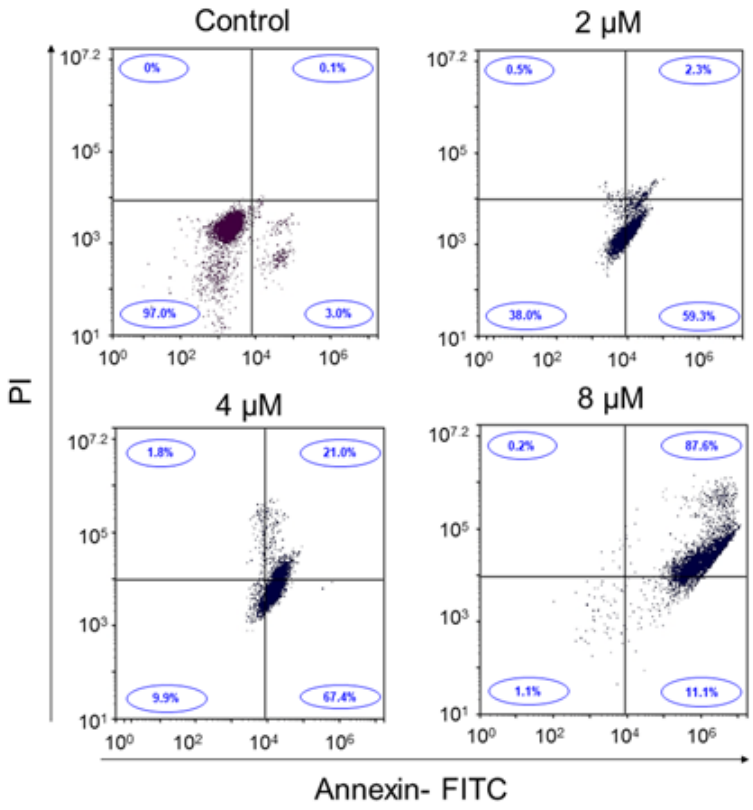

Figure S11 Apoptosis profiles of A549 cells after treatment with N770-DOX@NPs. Incubation time was fixed at 4 h at various N770 concentrations (0, 4, 6, and 8 μM) in the presence of laser irradiation (1.5 W/cm^2, 5 min).

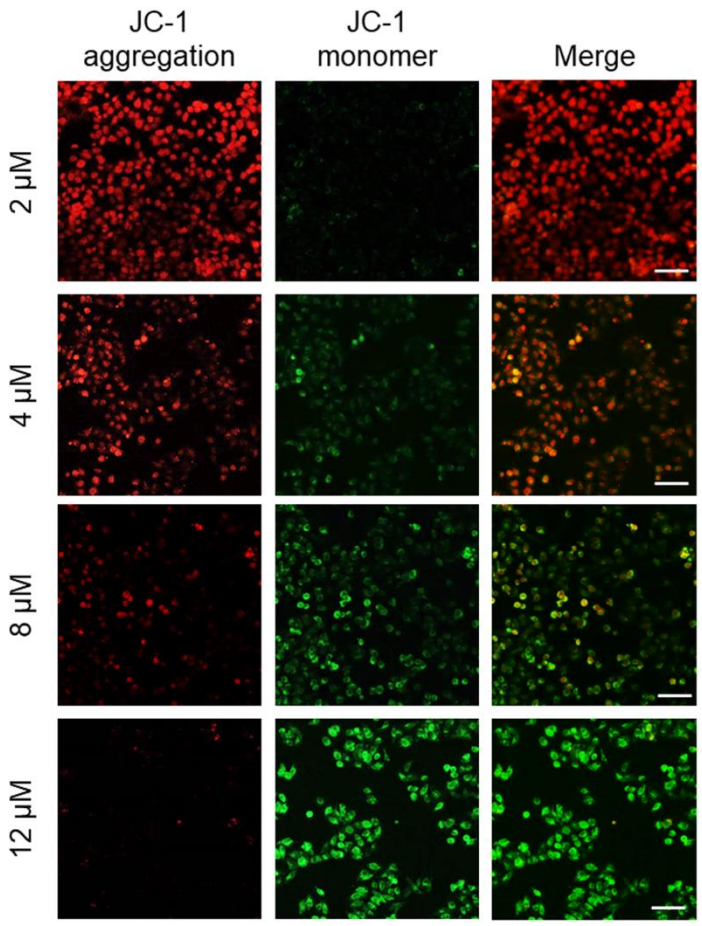

Figure S12 Mitochondrial damage analysis of A549 cells treated with N770-DOX@NPs (+NIR), and further stained with JC-1 fluorescent probes. Incubation time was fixed at 4 h at various N770 concentrations (0, 4, 6, and 8 μmol/L) in the presence of laser irradiation (1.5 W/cm^2, 5 min). Scale bar is 50 μm.

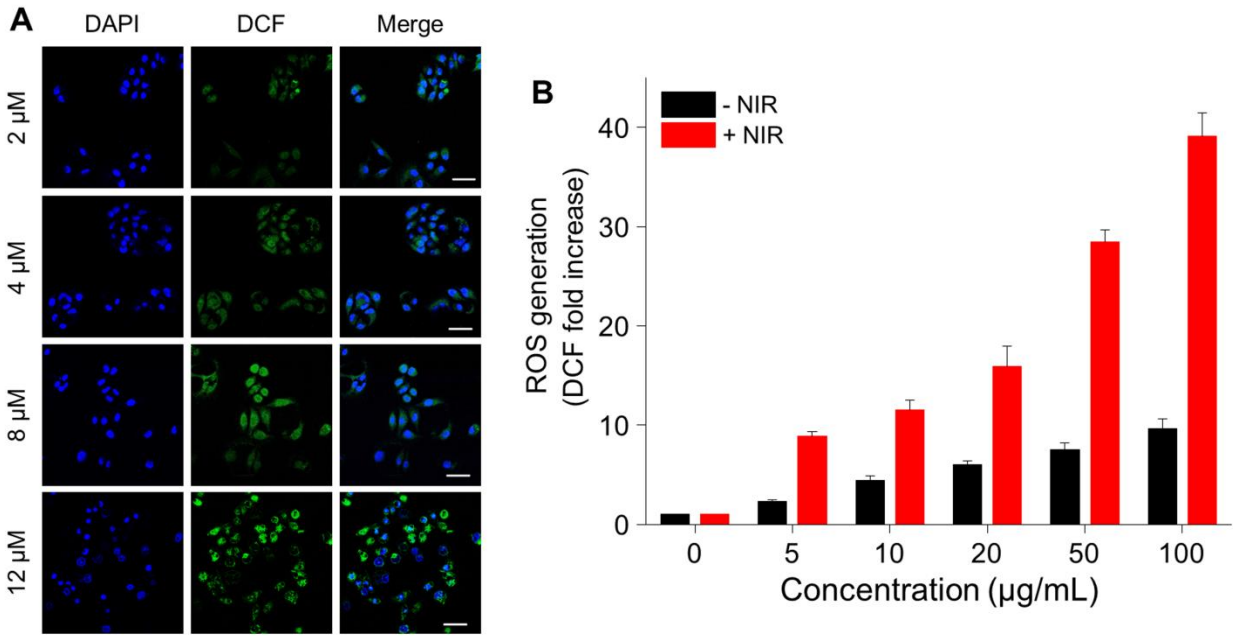

Figure S13 (A) Confocal images and (B) the quantitative results of intracellular ROS generation profiles of A549 cells treated with N770-DOX@NPs (+NIR), and further stained with DCFH-DA fluorescent probes. Nuclei were stained with DAPI (blue). Scale bar is 20 μm.

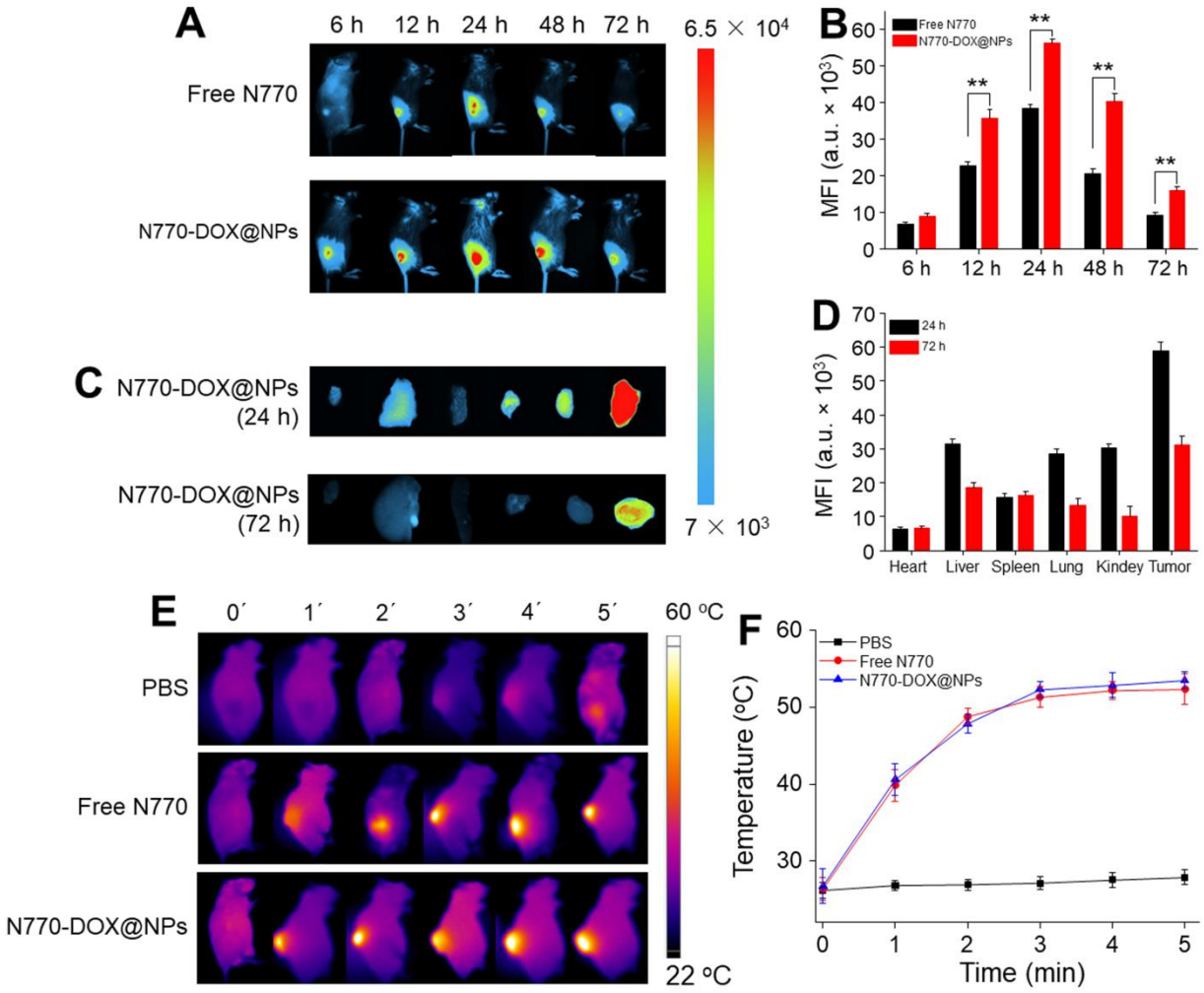

Figure S14*In vivo* bio-distribution of NPs in mice bearing 4T1 breast carcinoma xenografts. (A) FLI of mice bearing 4T1 tumor after intravenous injection of free N770 solution and N770-DOX@NP suspension at an equal N770 concentration of 1 mg/kg. (B) MFIs of tumor tissues from mice after treatment with free N770 and N770-DOX@NPs at different timepoints (6, 12, 24, 48, and 72 h). Data are expressed as mean ± SEM (n = 3; *, P < 0.05; **, P < 0.01; and ns = not significant). (C) *Ex vivo* FLI and (D) corresponding quantitative data of fluorescence intensities in the five major organs and tumor tissues from mice after the treatment with N770-DOX@NPs (N770: 1 mg/kg) at the timepoints of 24 and 72 h. Data are expressed as mean ± SEM (n = 3; *, P < 0.05; **, P < 0.01; and ns = not significant). (E) PTI of mice bearing 4T1

tumor after intravenous injection of free N770 solution and N770-DOX@NP suspension at an equal N770 concentration of 1 mg/kg for 24 h upon 808 nm laser irradiation (5 min, 0.8 W/cm^2), and (F) the temperature profiles of tumors monitored by infrared thermal camera. Data are expressed as mean ± SEM (n = 3).

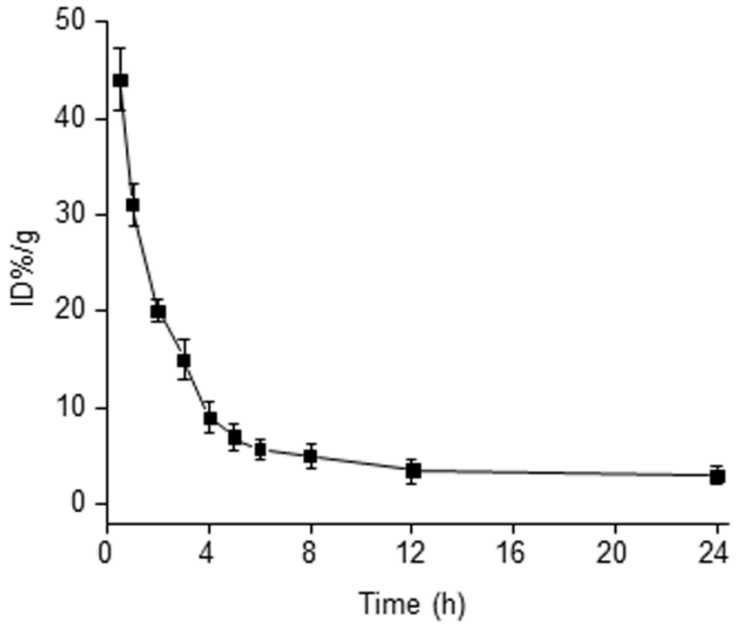

Figure S15 Variation of DOX concentrations in serum from mice bearing A549 lung carcinoma xenografts, which were intravenously injected with an N770-DOX@NP suspension at a DOX concentration of 1.41 mg/kg. Data are expressed as mean ± SEM (n = 3).

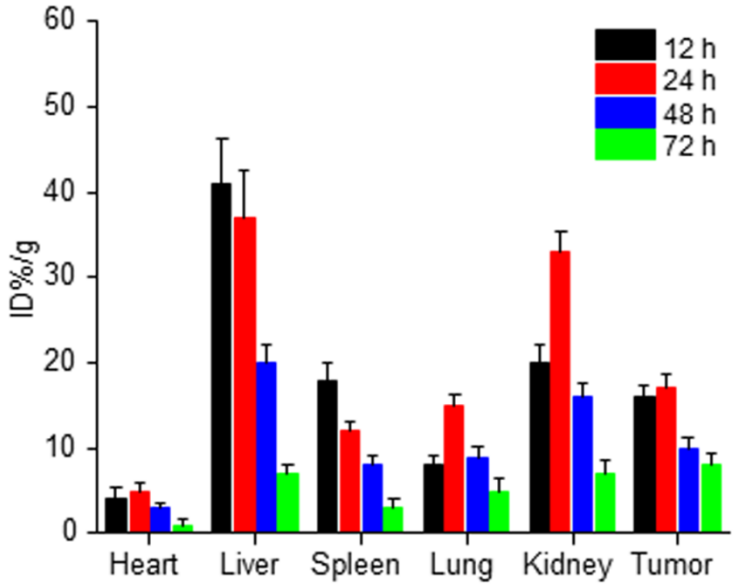

Figure S16 Quantification of DOX amounts in the major organs and tumor tissues of mice bearing A549 lung carcinoma xenografts, which were intravenously injected with DOX@NPs. Data are expressed as mean ± SEM (n = 3).

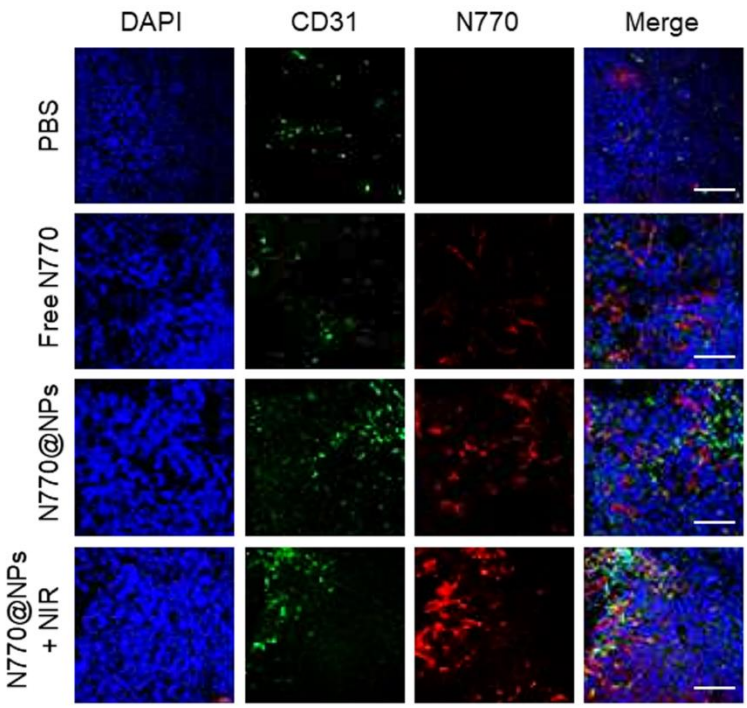

Figure S17 Immunofluorescence imaging of tumor slices from the mice receiving the treatment of PBS, free N770, N770@NPs, and DOX@NPs (+NIR). Nuclei were stained with DAPI (blue), and the tumor blood vessels were stained with CD31 antibody (green). Scale bar is 50 μm.

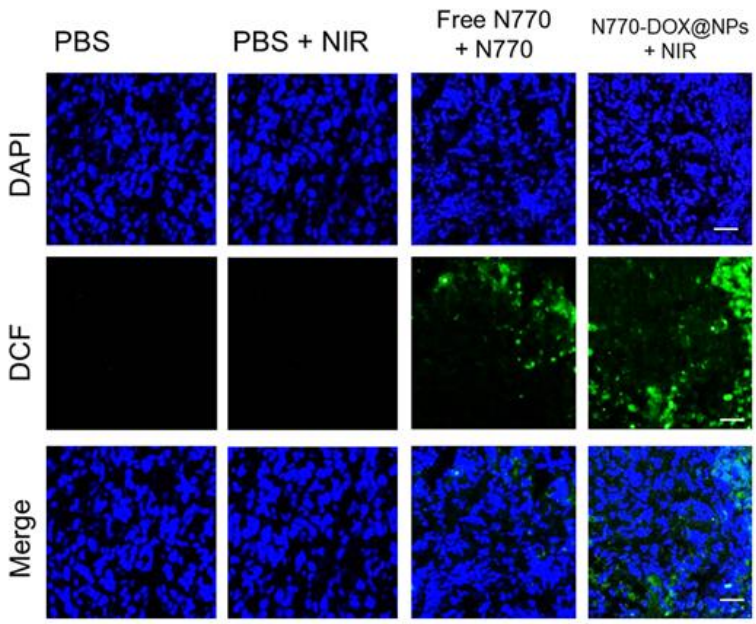

Figure S18 Confocal images of intracellular ROS generation profiles of A549 tumor tissues from mice treated with PBS (+NIR), free N770 (+NIR), and N770-DOX@NPs (+NIR), and stained with DCFH-DA fluorescent probes. Nuclei were stained with DAPI (blue). Scale bar is 50 μm.

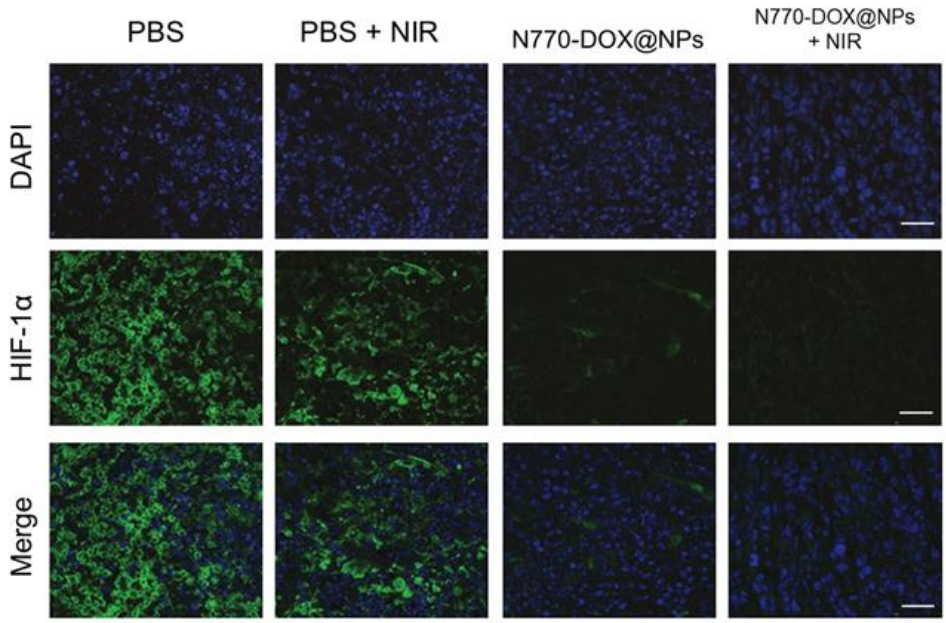

Figure S19 Immunofluorescence analysis of HIF-α expression profiles in A549 tumor tissues from mice in the groups treated with PBS (+NIR), free N770 (+NIR), and N770-DOX@NPs (+NIR). Nuclei were stained with DAPI (blue). Scale bar is 50 μm.

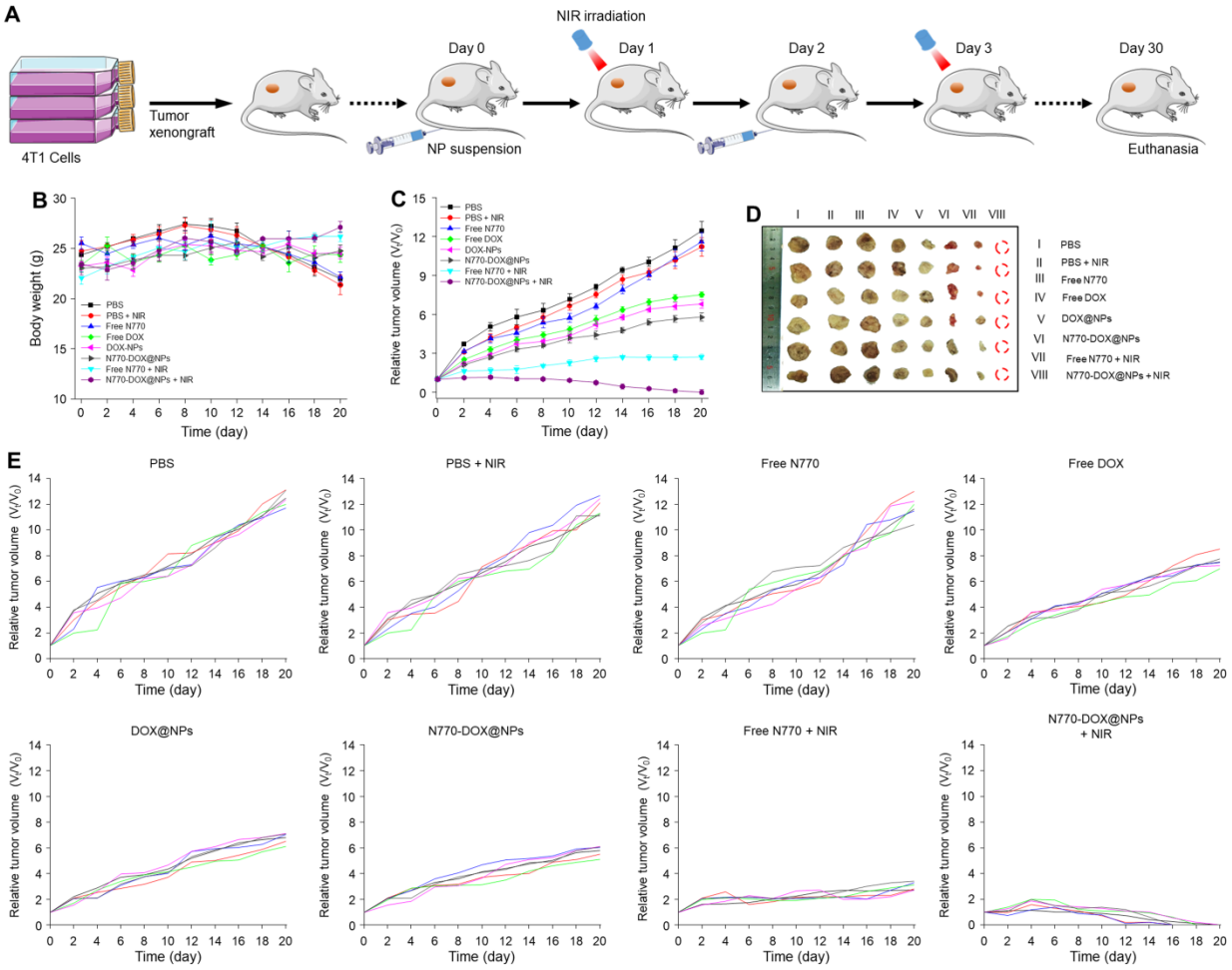

Figure S20 *In vivo* anti-cancer outcomes of NPs in the 4T1 breast tumor xenograft mouse model. (A) Schematic illustration of the treatment processes. (B) Body weight changes and (C) tumor growth curves of mice bearing 4T1 breast carcinoma xenografts. Data are expressed as mean ± SEM (n = 6). (D) Photographic images of tumors from the various treatment groups at the end of experiments. (E) Individual tumor growth profiles of mice from the various treatment groups.

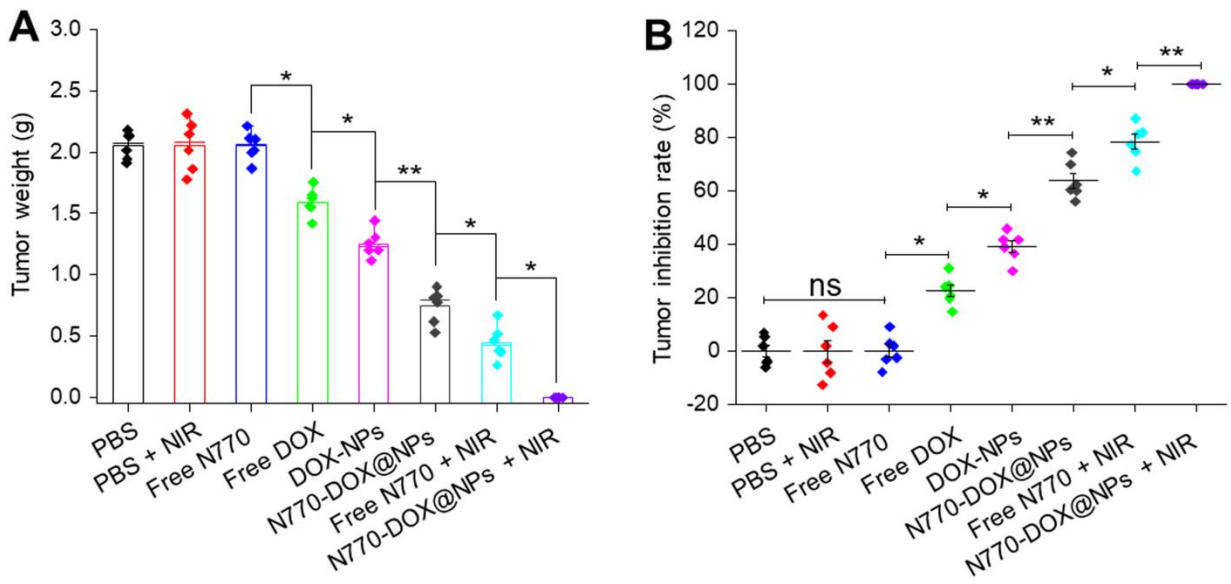

Figure S21 (A) Tumor weights and (B) tumor inhibition rates of 4T1 breast tumor-carrying mice from the various treatment groups. Data are expressed as mean ± SEM (n = 6; *P < 0.05; **P < 0.01; and ns = not significant).

Figure S22 Photographs of dissected lungs from 4T1 breast tumor-carrying mice receiving various treatments. Yellow dots indicate nodules.

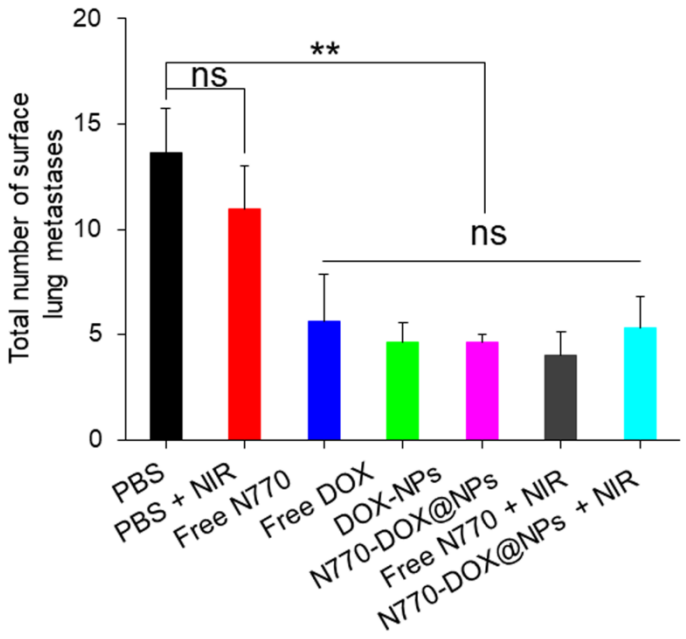

Figure S23 Number of lung metastatic nodules in 4T1 breast tumor-carrying mice receiving various treatments. Data are expressed as mean ± SEM (n = 6; *P < 0.05; **P < 0.01; and ns = not significant).

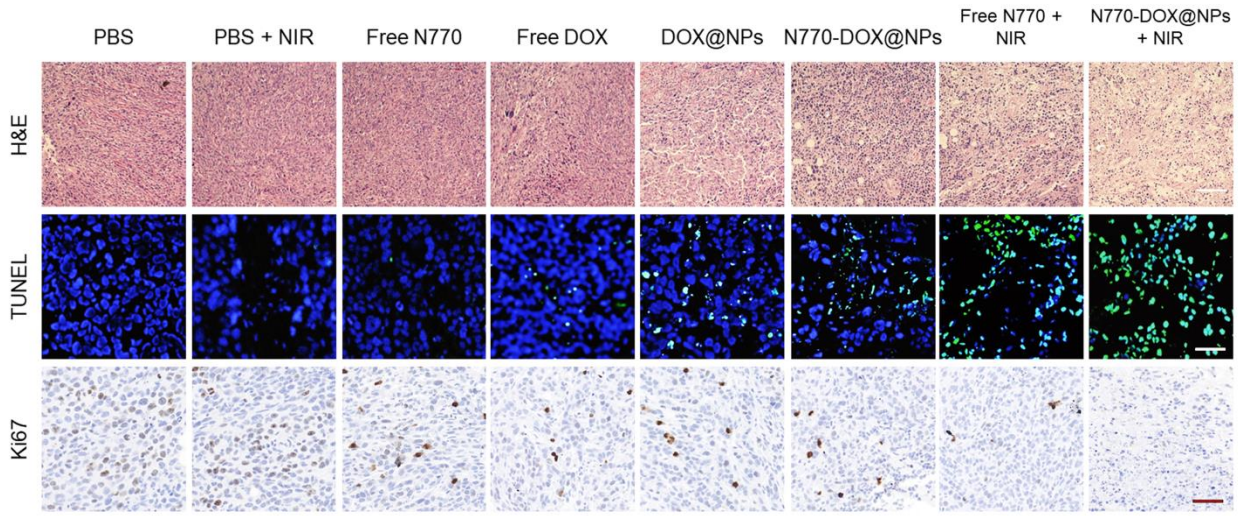

Figure S24 H&E staining, TUNEL staining, and Ki67 staining of tumor sections from 4T1 breast tumor-beared mice receiving various treatments. Scale bar represents 50 μm.

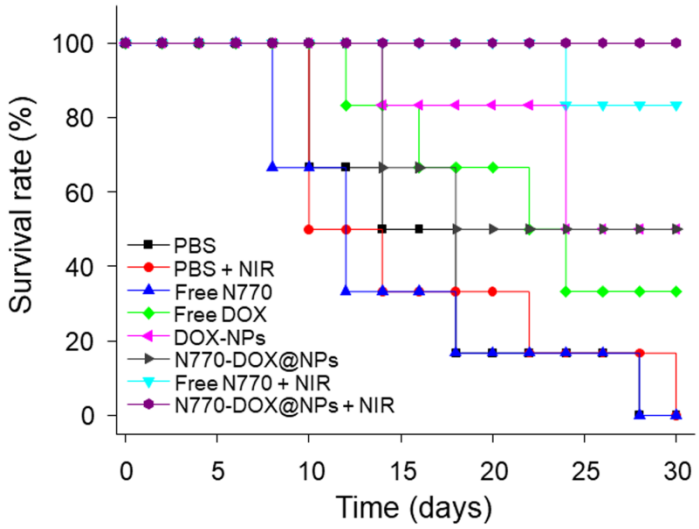

Figure S25 Survival rates for 4T1 breast tumor-carrying mice receiving various treatments (six mice in each group).

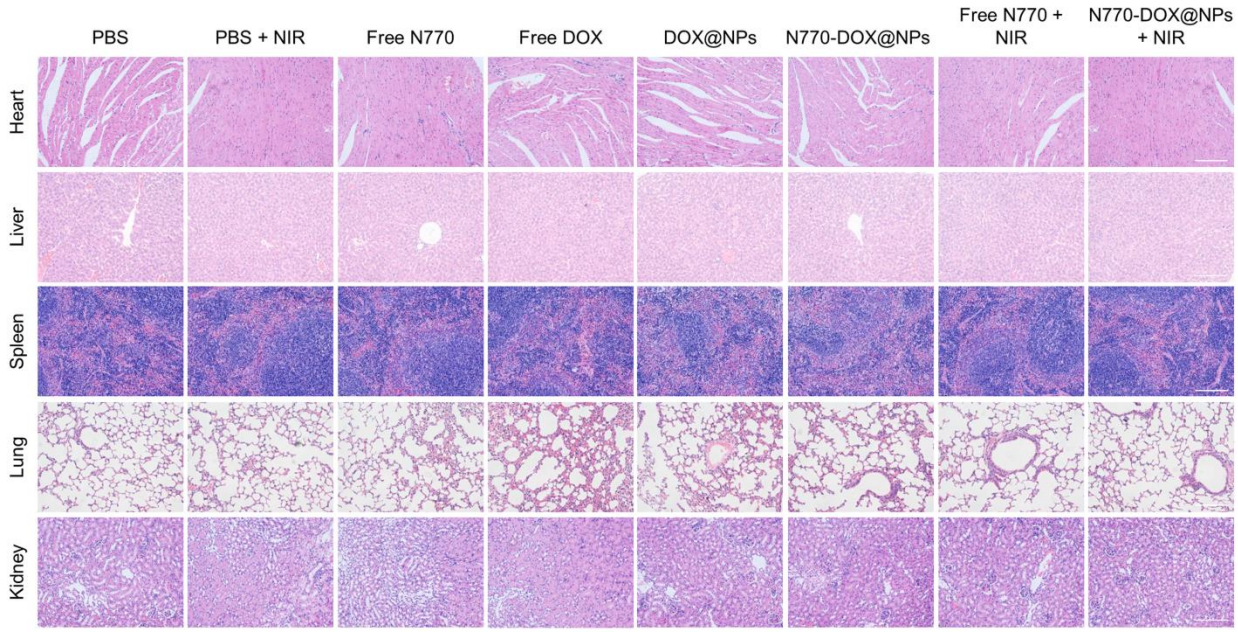

Figure S26 H&E staining of the five major organs (heart, liver, spleen, lung, and kidney) from PDX mice receiving various treatments. Scale bar is 200 μm.

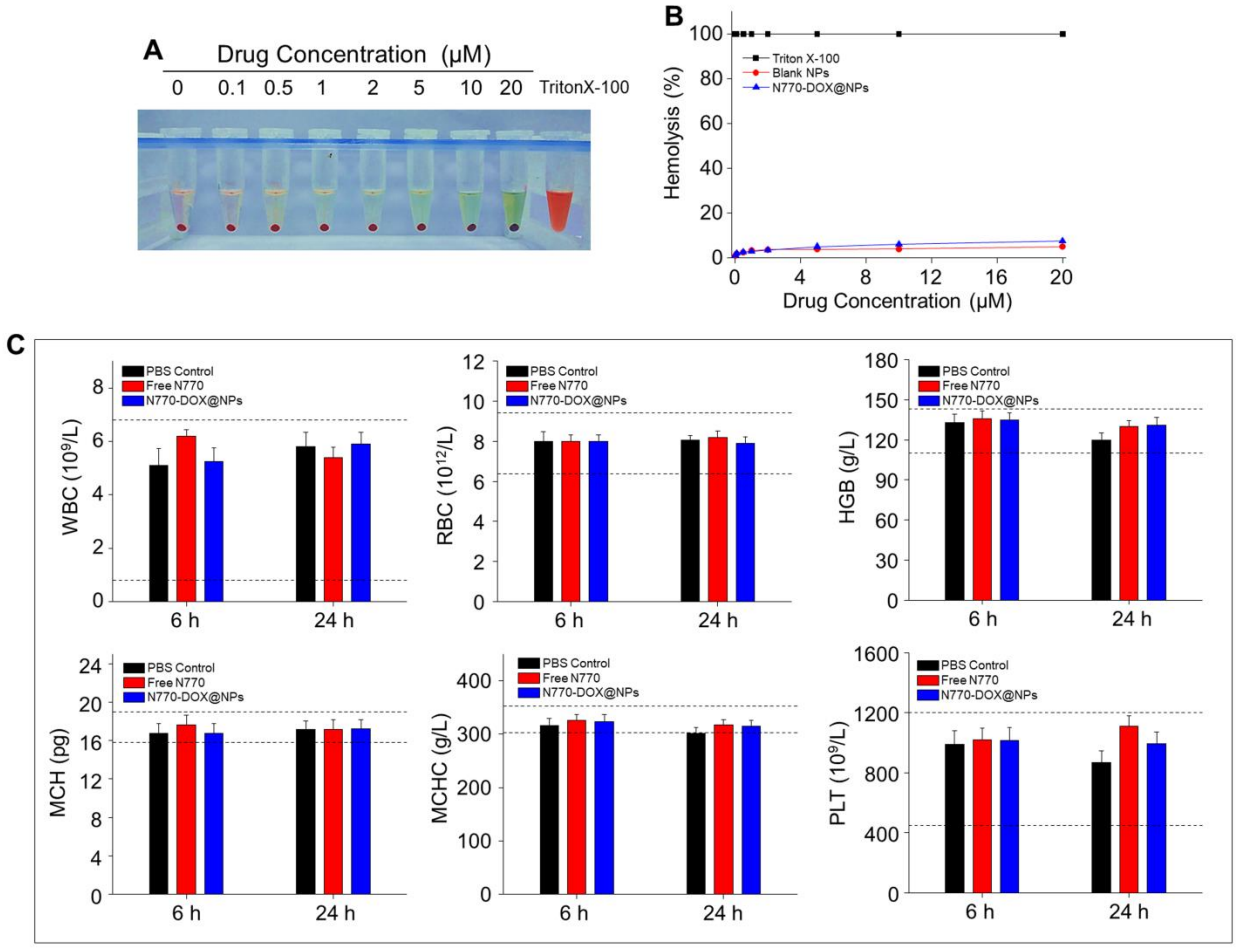

Figure S27 Hemocompatibility of N770-DOX@NPs. (A) Photograph of erythrocyte suspensions with different treatments. (B) Hemolytic analysis of different concentrations of NPs. Triton X-100 (1%, *w*/*v*) was used as a positive control (100%), whereas PBS was used as a negative control (0%). Data are expressed as mean ± SEM (n = 5). (C) Complete blood counts of typical parameters, including WBC, RBC, HGB, MCH, MCHC, and PLT.

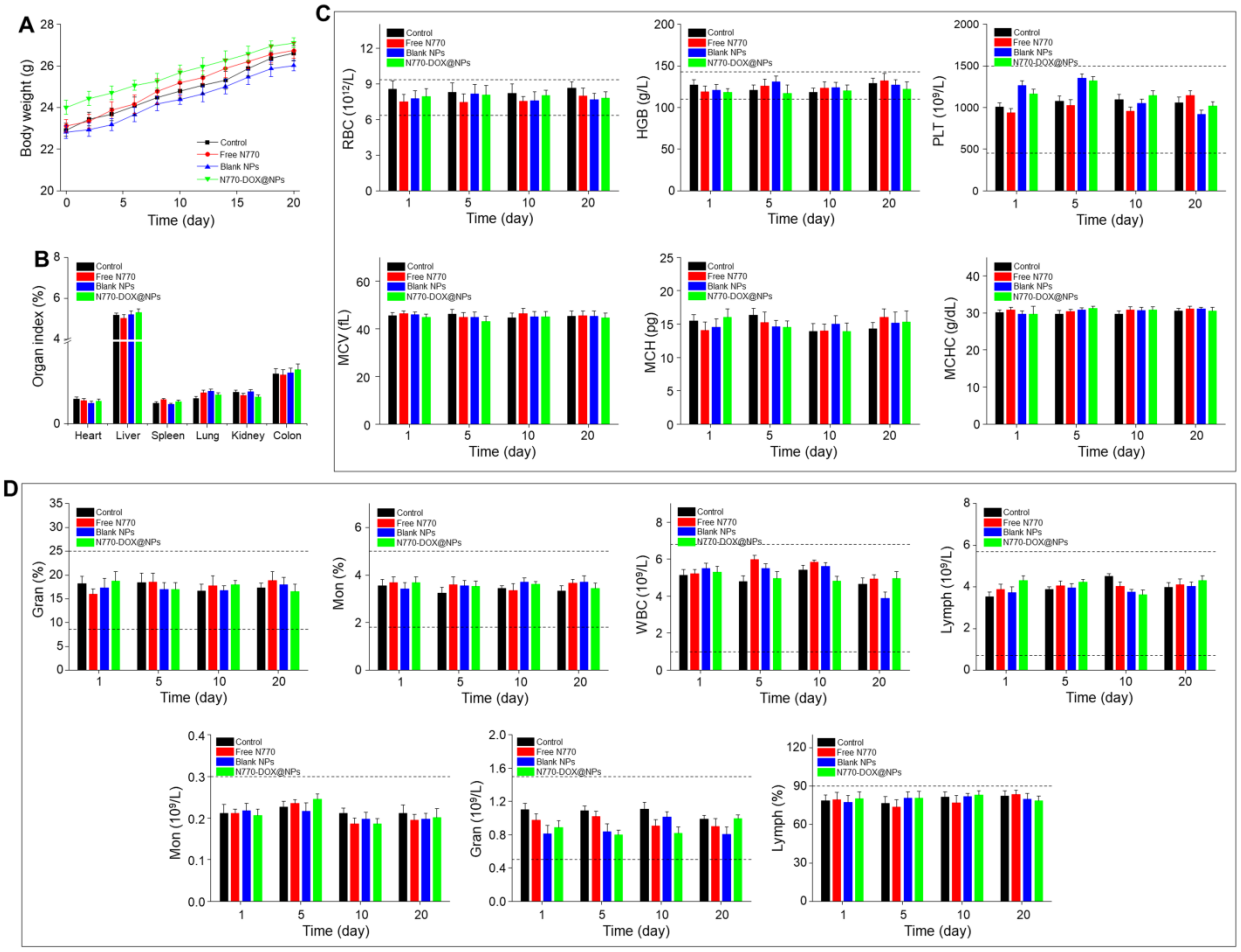

Figure S28 *In vivo* biosafety of N770-DOX@NPs. (A) Changes in body weight and (B) organ indices of mice treated with free N770, blank NPs, or N770-DOX@NPs. (C) Changes in complete blood counts of various blood factors over time. Data are expressed as mean ± SEM (*n* = 3).

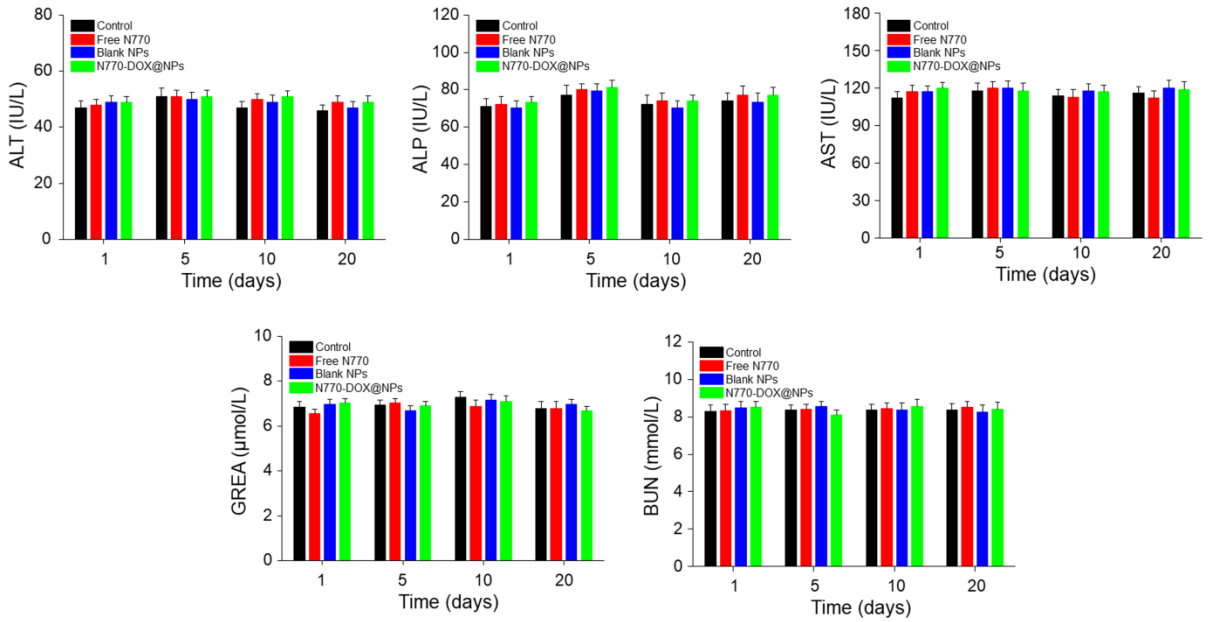

Figure S29 Typical biomarker molecules related to liver (ALT, ALP, and AST) and kidney functions (CREA and BUN). Data are expressed as mean ± SEM (n = 3).

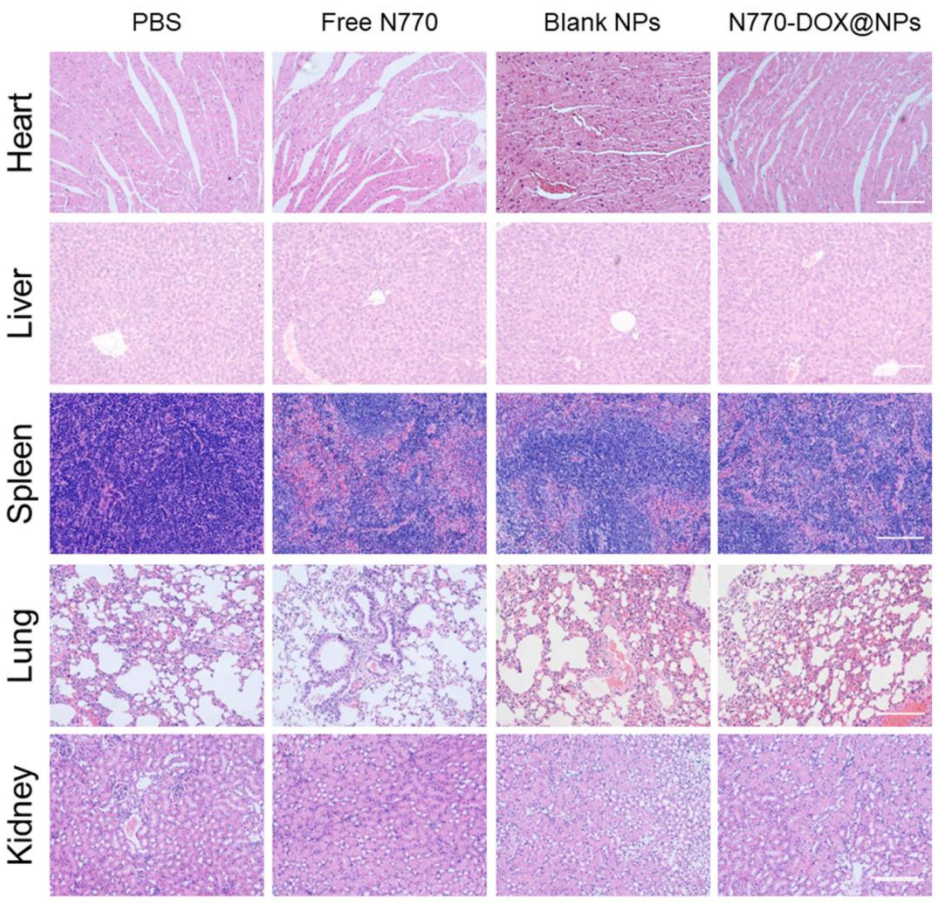

Figure S30 H&E staining of the five major organs (heart, liver, spleen, lung, and kidney) from mice receiving various treatments. Scale bar is 200 μm.

Table S1 Characteristics of various NPs.
Data are mean ± SEM; *n*=3. NPs, nanoparticles; PDI, polydispersity index; DOX, doxorubicin.

NPs	Diameter (nm)	PDI	Zeta potential (mV)	Loading amount (DOX)	Encapsulation efficiency (DOX)	Graft amount (N770)	Graft efficiency (N770)
Blank NPs	121.0	0.034	-13.7	-	-	-	-
DOX-NPs	124.2	0.052	-13.0	3.1%	74%	-	-
N770-DOX@NPs	157.4	0.101	-25.7	3.1%	74%	27.6 μg/mg	87.3%

Table S2 IC_{50} of various NPs against A549 cells and 4T1 cells.

NPs	IC_{50} (μg/mL)	
	A549 cells	4T1 cells
Free N770	1202.1	1320.7
Free DOX	7.4	6.9
DOX@NPs	212.4	201.2
N770-DOX@NPs	105.2	115.6
Free N770 (+NIR)	50.8	61.3
N770-DOX@NPs (+NIR)	15.6	17.1

NPs, nanoparticles; DOX, doxorubicin; NIR, near-infrared.

References

1. Zhu SJ, Hong MH, Tang GT, Qian LL, Lin JY, Jiang YY, et al. Partly PEGylated polyamidoamine dendrimer for tumor-selective targeting of doxorubicin: The effects of PEGylation degree and drug conjugation style. *Biomaterials* 2010;**31**:1360-71.

2. Al-Abd AM, Kim NH, Song SC, Lee SJ, Kuh HJ. A simple HPLC method for doxorubicin in plasma and tissues of nude mice. *Arch Pharm Res* 2009;**32**:605-11.